NASA/TM-2007-214544

Compact Ozone Lidar for Atmospheric Ozone and Aerosol Measurements

Joel Marcia
Old Dominion University, Norfolk, Virginia

Russell J. De Young
Langley Research Center, Hampton, Virginia

March 2007

The NASA STI Program Office . . . in Profile

Since its founding, NASA has been dedicated to the advancement of aeronautics and space science. The NASA Scientific and Technical Information (STI) Program Office plays a key part in helping NASA maintain this important role.

The NASA STI Program Office is operated by Langley Research Center, the lead center for NASA's scientific and technical information. The NASA STI Program Office provides access to the NASA STI Database, the largest collection of aeronautical and space science STI in the world. The Program Office is also NASA's institutional mechanism for disseminating the results of its research and development activities. These results are published by NASA in the NASA STI Report Series, which includes the following report types:

- TECHNICAL PUBLICATION. Reports of completed research or a major significant phase of research that present the results of NASA programs and include extensive data or theoretical analysis. Includes compilations of significant scientific and technical data and information deemed to be of continuing reference value. NASA counterpart of peer-reviewed formal professional papers, but having less stringent limitations on manuscript length and extent of graphic presentations.

- TECHNICAL MEMORANDUM. Scientific and technical findings that are preliminary or of specialized interest, e.g., quick release reports, working papers, and bibliographies that contain minimal annotation. Does not contain extensive analysis.

- CONTRACTOR REPORT. Scientific and technical findings by NASA-sponsored contractors and grantees.

- CONFERENCE PUBLICATION. Collected papers from scientific and technical conferences, symposia, seminars, or other meetings sponsored or co-sponsored by NASA.

- SPECIAL PUBLICATION. Scientific, technical, or historical information from NASA programs, projects, and missions, often concerned with subjects having substantial public interest.

- TECHNICAL TRANSLATION. English-language translations of foreign scientific and technical material pertinent to NASA's mission.

Specialized services that complement the STI Program Office's diverse offerings include creating custom thesauri, building customized databases, organizing and publishing research results ... even providing videos.

For more information about the NASA STI Program Office, see the following:

- Access the NASA STI Program Home Page at ***http://www.sti.nasa.gov***

- E-mail your question via the Internet to help@sti.nasa.gov

- Fax your question to the NASA STI Help Desk at (301) 621-0134

- Phone the NASA STI Help Desk at (301) 621-0390

- Write to:
  NASA STI Help Desk
  NASA Center for AeroSpace Information
  7115 Standard Drive
  Hanover, MD 21076-1320

NASA/TM-2007-214544

Compact Ozone Lidar for Atmospheric Ozone and Aerosol Measurements

Joel Marcia
Old Dominion University, Norfolk, Virginia

Russell J. De Young
Langley Research Center, Hampton, Virginia

National Aeronautics and
Space Administration

Langley Research Center
Hampton, Virginia 23681-2199

March 2007

Available from:

NASA Center for AeroSpace Information (CASI)
7115 Standard Drive
Hanover, MD 21076-1320
(301) 621-0390

National Technical Information Service (NTIS)
5285 Port Royal Road
Springfield, VA 22161-2171
(703) 605-6000

ABSTRACT

A small compact ozone differential absorption lidar capable of being deployed on a small aircraft or unpiloted atmospheric vehicle (UAV) has been tested. The Ce:LiCAF tunable UV laser is pumped by a quadrupled Nd:YLF laser. Test results on the laser transmitter demonstrated 1.4 W in the IR and 240 mW in the green at 1000 Hz. The receiver consists of three photon-counting channels, which are a far field photomultiplier tube (PMT), a near field UV PMT, and a green PMT. Each channel was tested for their saturation characteristics.

1.0 INTRODUCTION

Climate and air quality are important subjects that affect economy, productivity and quality of life. A sudden change in the weather can delay a casual outing or endanger a multibillion-dollar project. Subsequently, climate and air quality have become increasingly important and this has motivated an increase need for fundamental atmospheric measurements.

One of the major issues that can have a dramatic effect on our weather is global warming, which can no longer be ignored. In the past several years, global warming has been an important topic in many political arenas, the scientific community, and the general public. A tremendous amount of speculation exists as to what can happen if global warming goes unchecked, anywhere from very little change to a global catastrophe. More information needs to be gathered to increase our knowledge and understanding of this global issue and how it will continue to affect us.

Likewise, air quality has become a major issue. Our quality of life can be greatly reduced if air pollution goes unchecked. World governments are becoming more aware of air pollution and are passing legislation to regulate the amount of air pollution released into the air. Air pollution can have an adverse affect on health especially those with respiratory and pulmonary health problems.

To get a better understanding of global warming, climate, and air quality it is necessary to take a closer look at the Earth's atmosphere. The Earth's atmosphere is a mixture of water vapor, particles (aerosols), and gases surrounding the planet. A delicate balance must be preserved in order for the air to continue to support life on the planet. The atmosphere consists mainly of nitrogen and oxygen. Many other gases and aerosols are also contained within the atmosphere, for example argon, carbon dioxide, and ozone (O_3). An important area of concern is ozone and its effect on air quality. Manmade ozone is also one of the "greenhouse" gases that contributes to global warming. It is important to determine the location, distribution, and the effect of ozone on the planet's atmosphere.

Ozone is normally found within the Earth's atmosphere at two different altitudes known as the troposphere and stratosphere. The troposphere is located from the ground up to an altitude of about 10 km and the stratosphere, with a higher concentration of ozone, is found at an altitude from 10 to 50 km[1,2]. Above the troposphere is the

stratosphere where ozone protects the Earth by absorbing most of the dangerous ultraviolet radiation from the sun[2].

Unfortunately, chlorofluorocarbons (CFCs), which are used as a refrigerant and found in aerosol products, can deplete the stratospheric ozone. When ultraviolet radiation breaks down a CFC molecule, a chlorine atom is released and can destroy as many as 100,000 ozone molecules in the stratosphere[3].

When nitrogen dioxide (NO_2) is released into the troposphere, normally by industrial plants and cars, it forms ozone affecting air quality. A known pollutant NO_2 is excited by solar radiations and converted into nitric oxide (NO). This process releases oxygen (O) that is free to combine with atmospheric oxygen molecules (O_2) to produce the ozone found near the Earth's surface. Tropospheric ozone is one of the key ingredients of smog reducing air quality and one of the contributors to the greenhouse effect that causes global warming[4].

1.1 LIDAR AND THE DIAL METHOD TO MEASURE ATMOSPHERIC OZONE

In order to help predict and possibly prevent future global warming and improve air quality, it is important to know the concentration and the distribution of ozone in the atmosphere. The use of Light Detection And Ranging or lidar has been widely used in the study of atmospheric measurements of gas and aerosol concentrations. Lidar uses the same principle as RADAR. When a pulsed lidar system transmits light to a target, the light interacts with the target and the light is scattered or reflected back to a receiver within the lidar system. Since the speed of light is known (~$3x10^8$ m/s), the round trip time between the emitted pulse and its return to the receiver determines the distance to the atmospheric target.

A specific type of lidar known, as Differential Absorption Lidar (DIAL) is a technique that has been successful in measuring chemical concentrations found in the atmosphere such as water vapor, pollutants, gases, and ozone[7]. Different molecules absorb light only at specific wavelengths. Based on this concept, a two-wavelength differential absorption technique is used, one wavelength (on-line) is chosen where a gas absorbs that particular wavelength and the second wavelength (off-line) in which the gas does not absorb is used as a reference. For example, when measuring O_3, taking the ratio of the two signals and using well-known absorption coefficients of ozone, the concentration of O_3 is calculated from the differential absorption. By employing ratios, the scattering contributed by aerosols is eliminated, while acquiring the differential absorption due to ozone[5].

In June 2000, a compact DIAL ozone lidar system was designed and constructed by Science and Engineering Services, Inc. (SESI) for atmospheric ozone and aerosol measurements. This system was delivered to the Air Force and used at Dryden AFB, CA for measuring ozone from the ground. It was subsequently then given to NASA Langley in 2003 for use as a compact ozone lidar measurement system. The purpose of this research effort is to characterize and make operational this compact lidar system. This system will eventually be deployed for aircraft, and possibly unpiloted atmospheric vehicle (UAV), based ozone and aerosol measurements to improve our understanding of ozone production and transport.

2.0 SYSTEM DESCRIPTION

The compact DIAL lidar system consists of several components, as shown in figure 1. These components are divided into three primary subsystems: the laser transmitter, the receiver, and the system control rack, which houses the data acquisition and the lidar control.

2.1 LIDAR TRANSMITTER

In the following paragraphs, the main components of the laser transmitter system and its support units are discussed. The transmitter module itself is enclosed in a rectangular box (17.5cm x 46cm x 104 cm) and the support units (power, control and cooling) are located on the system rack.

A control unit maintains the transmitter system and houses the power supply for the lasers, the amplifiers, and the acousto-optic Q-switch. Also enclosed in the control unit are the temperature controls for the LBO doubling and CLBO quadrupling crystals as well as the visual indicators for laser emission and the laser shutter.

The first main component of the transmitter shown in Figure 2 is a tunable Ce:LiCAF laser custom built by SESI . It has digital wavelength tuning and temperature control. The Ce:LiCAF laser has an output wavelength range of 280 to 320 nm with a maximum pulse repetition rate of 1 kHz. By using a single tunable laser to produce the two required wavelengths, size and cost are reduced[5]. As discussed earlier, DIAL measurements require two different wavelengths, in this case 288 nm and 293 nm. To produce two different wavelengths using a single laser, a rotating tuning mirror is mounted on a motorized rotary mount. Rotating this mirror chooses the desired wavelengths for ozone measurements.

The second element of the transmitter is a laser pump, for the Ce:LiCAF laser. The laser pump, Nd:YLF laser, is a modified Q-Peak Inc. (Model MPS-262 QS 20e) system. The laser pump starts with a diode-pumped Nd:YLF oscillator (refer to figure 2). Within the oscillator cavity are pump diodes, beam expander, Q-switch, and cavity mirror. Next are the amplifiers #1 and #2. The two dioded-pump Nd:YLF amplifiers are designed to increase the infra-red (IR) pulse energy. The last part of the laser pump consists of second and fourth harmonic converters. The frequency doubling LBO crystal converts ~50% of the infrared power generated into the second harmonic green radiation. Then the quadrupling CLBO crystal converts this second harmonic energy to UV, or the fourth harmonic. The output wavelength of the Nd:YLF laser pump and converters is 262 nm with an energy output of approximately 2 mJ per pulse at 1 kHz[5]. This then pumps the Ce:LiCAF crystal producing ~1.0 mJ at the desired ozone UV wavelengths. This beam (and the green) exits the transmitter and is directed to a motorized mirror in front of the telescope, which allows the beam to be aligned with the stationary telescope.

In order to maintain optimum temperature of the laser and its components, a cooling unit is employed. This unit contains a closed-loop system, which includes a coolant heat exchanger, an air-cooled refrigeration unit, and a recirculation pump.

2.2 LIDAR RECEIVER

The lidar receiver system consists of a 35 cm diameter Cassegrainian telescope (Celestron C-14) optimized for UV wavelengths and a detection array mounted behind the telescope. The diameter of the field of view aperture is 13 mm. The detection array employs three channels, the green aerosol and two UV channels (near- and far-field). After the signal is received from the telescope, the signal is divided into green and UV beams by a beam splitter, as shown in figure 3. The green and UV light are collimated. The UV signal is also filtered and divided into near-field and far-field channels by means of a beam splitter. For the on-line and off-line signals, two different filters are used and are continuously interchanged using a mechanical slide. Approximately 1-2% of the UV signal is sent to the near-field photomultiplier tube (PMT 1) manufactured by Hamamastu (R2949) and the remaining ~99% is sent to the far-field photomultiplier tube two (PMT 2) also manufactured by Hamamastu (R7207-01). The green signal is directed to PMT 3 manufactured by Electron Tubes Inc (P10PC). All the outputs from the PMTs go through a trans-impedance amplifier and a level discriminator to produce TTL pulses related to the light intensity. Multi-channel scaler cards (Perkin Elmer MCS), one for each channel, digitally process the TTL pulses and stores them on a hard disk.

2.3 DATA ACQUISITION AND LIDAR CONTROL

Several components are used in data acquisition and lidar control. A schematic of the complete lidar system can again be found in figure1. An industrial computer is used for data acquisition, analysis, and control. A SESI custom designed General Control Unit (GCU) module controls lidar operations and data acquisition. The GCU contains a master clock for the timing sequences of the following: the laser, the switching between the on-line and off-line wavelengths, the data acquisition system, and the operation of the energy monitors. The DC power supplies for the three photomultiplier tubes (PMT 1, PMT 2, and PMT 3) are also contained in the GCU.

2.4 ATMOSPHERIC SETUP

A basic diagram of the atmospheric setup is shown in figure 4, and a photo of the complete system is shown in figure 5. To obtain an ozone atmospheric measurement, the transmitter sends a laser pulse into the atmosphere at the on-line wavelength for about 10 seconds then changes to the off-line wavelength. The 523 nm green laser output is always transmitted giving a return from atmospheric aerosols. The MCS units are used to accumulate the three signals for approximately 10 seconds. The telescope receives the scattered light from the atmosphere and the light is sent to the detection system to be processed. The computer analyses the data as well as displays and stores the results.

3.0 EXPERIMENT AND RESULTS

This section will describe test results of this lidar system in preparation for atmospheric lidar transmission.

3.1 TRANSMITTER LASER RESULTS

The initial test of the transmitter consisted of powering up the transmitter module to initially assess the problems with the transmitter. The Q-peak Laser Program was used to set the current values for the oscillator, amplifier #1, and amplifier #2 at 22A, 21A, and 18A respectively. A laser detector connected to an oscilloscope, was mounted behind the oscillator back mirror to measure and detect a laser pulse. A power meter was mounted in front of the LBO crystal to measure the power output of the Nd:YLF pump laser.

A large variance in the green output was observed as the temperature of the LBO crystal was adjusted. As a result, this had a large effect on the conversion efficiency. Using a laser power meter to measure the output of the green, the LBO crystal temperature knob was adjusted to optimize the output for maximum green energy. When stable, the full width at half maximum (FWHM) measurement of the IR laser pulse was approximately 26 ns.

A test was conducted to assess the IR output (1047 nm) power of the pump laser before the LBO crystal. The current settings of the oscillator, amplifier #1, and amplifier #2 were varied and the laser output power was measured at 1 KHz. First, the oscillator output power was recorded as the current was adjusted from 18 to 23 amps as shown in figure 6. The data revealed a linear relationship between the power output and the oscillator current. Second, while the oscillator current was held constant at 23 amps, the current for amplifier #1 was adjusted from 6 to 21 amps. The data is shown in figure 7. The data revealed an exponential trend in the gain as the current was increased in amplifier #1. The maximum gain is approximately ~ 8. Third, the oscillator and amplifier #1 current was held constant at 23 amps and 21 amps respectively as amplifier #2 was adjusted. The current of amplifier #2 was adjusted from 12 to 18 amps and the gain recorded as shown in figure 8. The max gain was ~ 5. As with amplifier #1, amplifier #2 produced an exponential trend in gain as the current was increased, but no saturation of the gain observed.

To measure the conversion efficiency of the LBO crystal, a laser power meter measured the input power (IR) and the output power (green) of the LBO crystal. The following current settings were used for the oscillator, amplifier #1 and #2: 23A, 23A, and 31A, respectively, and the repetition rate was set at 1000 Hz. The maximum power and energy for the IR and green were measured. The data is listed in table 1.

Table 1: The measured input and output power of the LBO crystal and its efficiency

Infrared (1047nm)	Green (524nm)
1.4 W	240 mW
Efficiency approximately 17%	

As seen in table 1, the efficiency of the second harmonic LBO crystal is approximately 17%. The efficiency of the second harmonic (LBO crystal) should have been approximately 50%[5], thus the input IR pulse energy needs to be greater since conversion efficiency is a nonlinear function of IR input energy.

3.2 RECEIVER EXPERIMENTAL RESULTS

Using the MCS Photon Counting Program, the receiver system was initially tested and evaluated. The detection system enclosure was examined and evaluated for external light leakage. Using a simple procedure, the enclosure was tested by running the PMTs with no input signal sent into the receiver. An excessive amount of external light was leaking into the enclosure. With a closer inspection of the enclosure, a significant amount of screws were missing. The detection enclosure was also opened to ensure the light blocking pads were in place. With the enclosure cover reinstalled, the enclosure was retested for external light leaks and no external light leaks were detected.

A formal test was conducted to test each of the three PMTs to determine the count rate in MHz that each tube saturates. As a PMT detector reaches the saturation point, the possibility of count error increases because of overlapping pulses. The maximum count rate depends on the minimum time interval, known as the pulse-pair resolution. The pulse-pair resolution is when two pulses cannot be resolved from each other[6]. To calculate the true count rate, the following equation was used[6].

$$N = \frac{M}{1 - M \cdot T} \qquad (1)$$

Where $N(s^{-1})$ is the true count rate, $M(s^{-1})$ is the measured count rate, and T(s) is the pulse-pair resolution (twice the individual pulse FWHM). The FWHM pulse measurements of each PMT were recorded and listed in table 2.

Table 2: The FWHM pulse measurements of each PMT

PMT 1 (Near-field UV)	PMT 2 (Far-field UV)	PMT 3 (Green)
9.2 ns	9.8 ns	5.6 ns

A pulsed xenon lamp (Perkin Elmer RSL-3100-10), which replicates a laser return pulse (a sample pulse profile is shown in figure 9), was used as the telescope input signal, as shown in figure 9. To achieve a specific range of light intensities, the xenon lamp was adjusted in small increments back and forth within the receiver. At each position, saturation measurements were recorded which consisted of taking two different measurements. The first measurement was recorded at full intensity of the xenon lamp. The second measurement required adding a neutral density filter in front of the xenon lamp to reduce the light intensity by $10^{0.5}$ (ND 0.5). Therefore, the data reflects two sets of measurements – one without the ND 0.5 filter and one with the ND 0.5 filter. Then a

ratio (R) was formed by dividing the count rate with no ND by the count rate with ND. No matter what the signal intensity input, this ratio should be constant until the detector saturates. To help increase the xenon output range, other neutral density adjustment filters were added as needed. Using equation 1, the true count rate was calculated for each measurement.

For each PMT, a graph was produced showing the R-ratio versus the count rate without the ND 0.5 filter as shown in figures 10. With each graph, there is a linear region with noticeable drop-off in the R-ratio at high-count rates. The drop-off point represents the maximum operating frequency for that particular PMT as the region above the maximum operating frequency is nonlinear. After this point, the PMT becomes saturated and can no longer provide accurate measurements. Table 3 listed the maximum operating count frequency for each PMT.

Table 3: The maximum operating frequencies for each PMT

PMT 1 (Near-field UV)	PMT 2 (Far-field UV)	PMT 3 (Green)
8 MHz	64 MHz	129 MHz

4.0 CONCLUSION

A compact ozone lidar system for use in measuring ozone in the atmosphere was tested in the laboratory. The receiver operated as expected and the maximum operating frequencies were determined for each photomultiplier tube. For the near-field UV PMT, the maximum count rate is 8 MHz. For the far-field UV PMT, the maximum count rate is 64 MHz, and for the green PMT, the maximum count rate is 129 MHz. Additionally, there was a low efficiency rating of approximately 17% measured for the LBO crystal which will require increasing the IR input energy. The IR from the oscillator, amplifier #1, and amplifier #2 was measured. A maximum gain for Amp. #1 was measured to be 8 and that from Amp. # 2 was 5. The maximum measured IR and green powers were 1.4 W and 240 mW, respectively. The laser pump IR was optimized to maximize the green energy just before the CLBO crystal, in order to get as much energy at 262 nm as possible to pump the Ce:LiCAF crystal.

The next step will be to insert the CLBO crystal and convert the green into UV energy in order to pump the Ce:LiCAF crystal thus producing the needed UV on and off line wavelengths to measure atmospheric ozone.

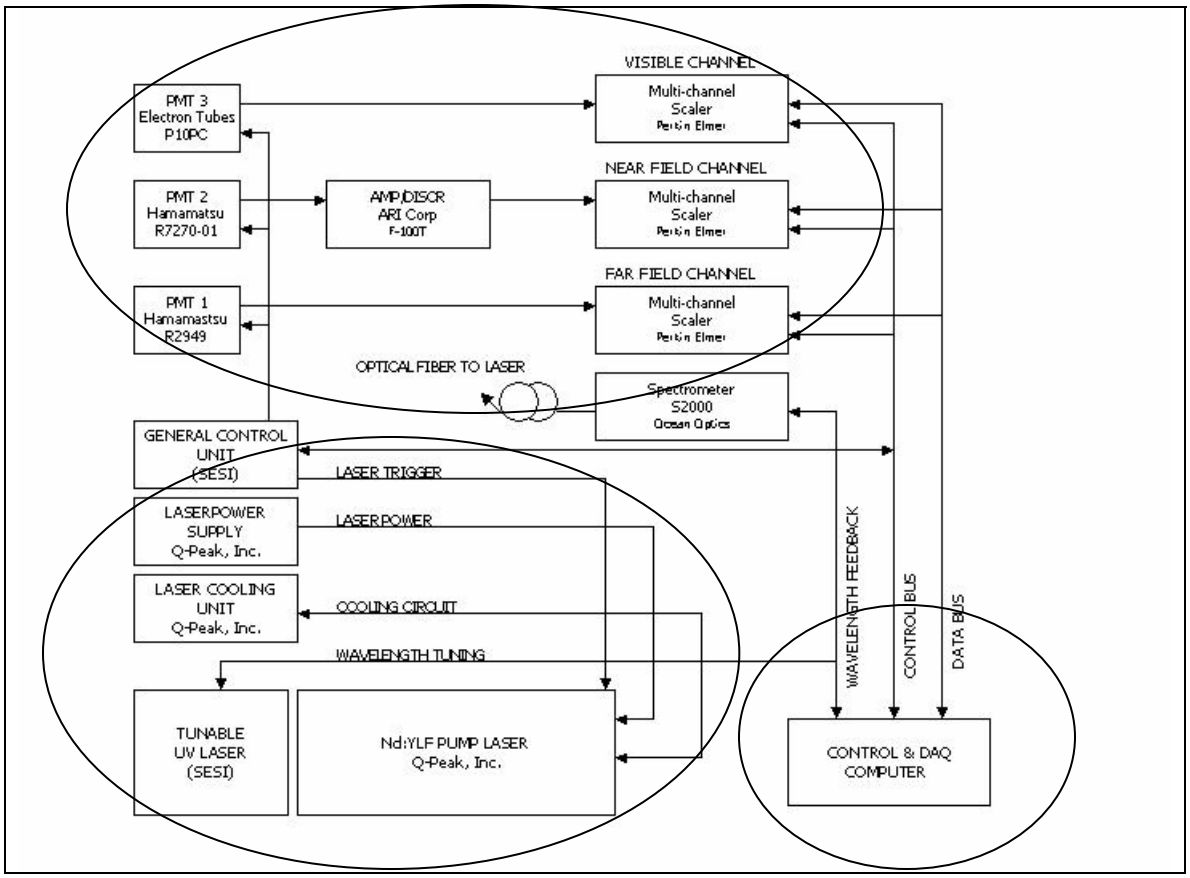

Figure 1: A schematic of the complete lidar system. The major components are top circle receiver, bottom circle laser transmitter and right circle control and data acquisition.

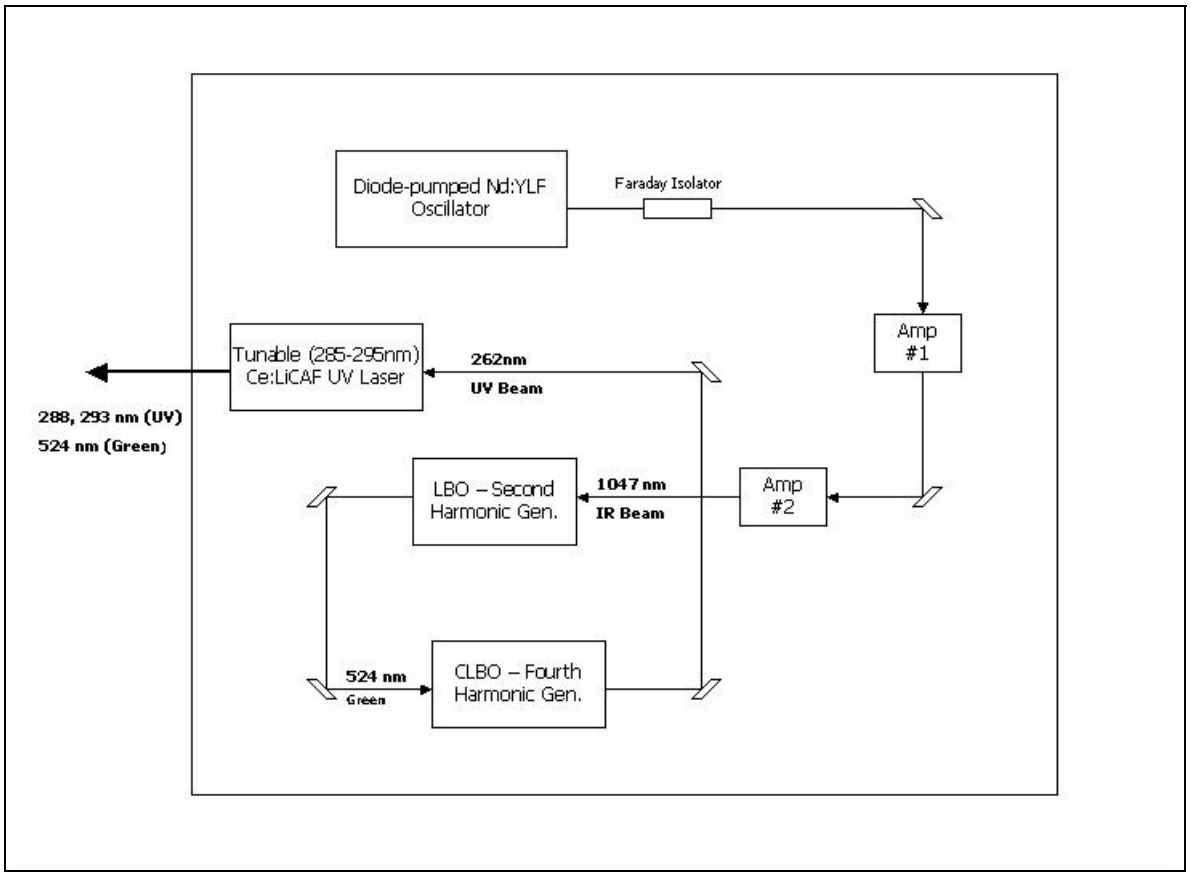

Figure 2: A schematic of the laser transmitter module which includes a laser pump and tunable laser.

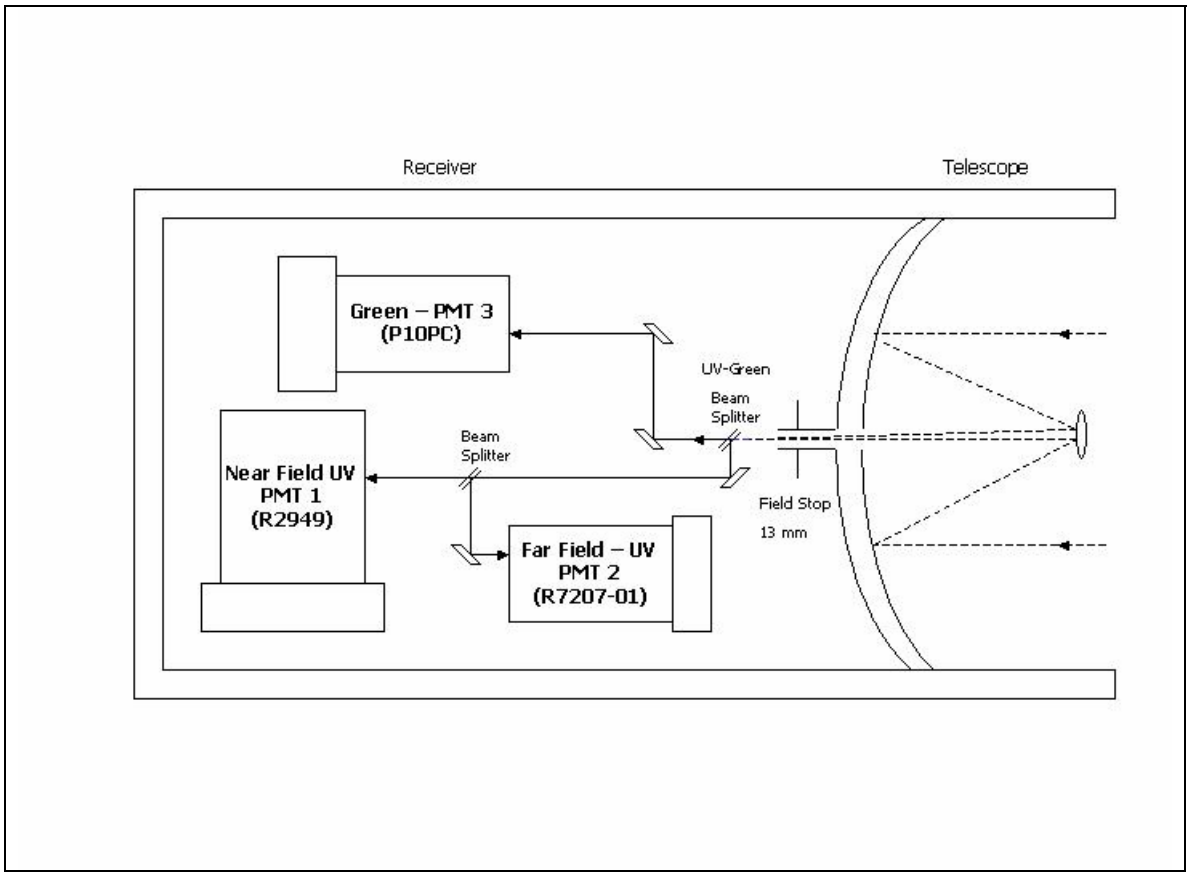

Figure 3. A schematic of the receiver system which includes a Celestron C-14 telescope and three photomultiplier tubes.

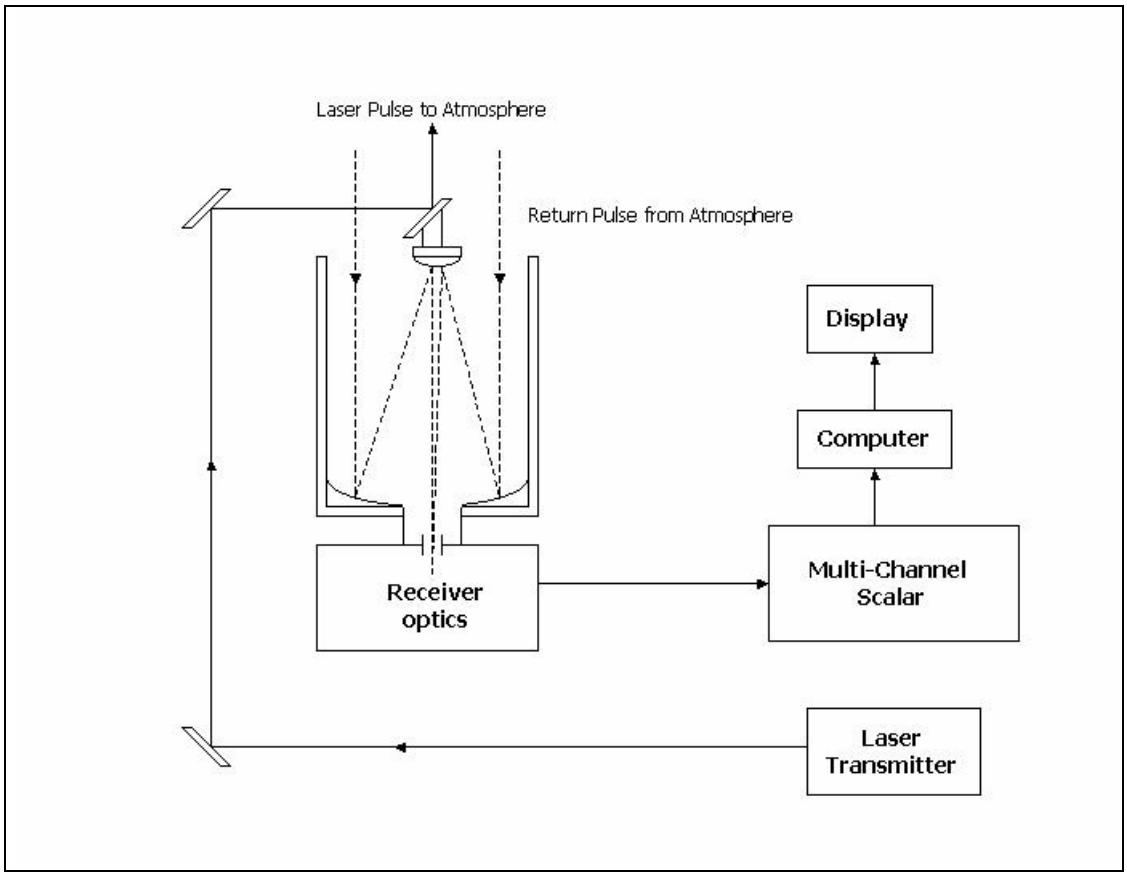

Figure 4. The laser transmitter sends a laser pulse into the atmosphere and the return pulse enters the receiver. The signal is processed and analyzed by the multi-channel scalar and computer respectively. Then the results are displayed.

Figure 5: A picture of the compact DIAL lidar system taken within the lab.

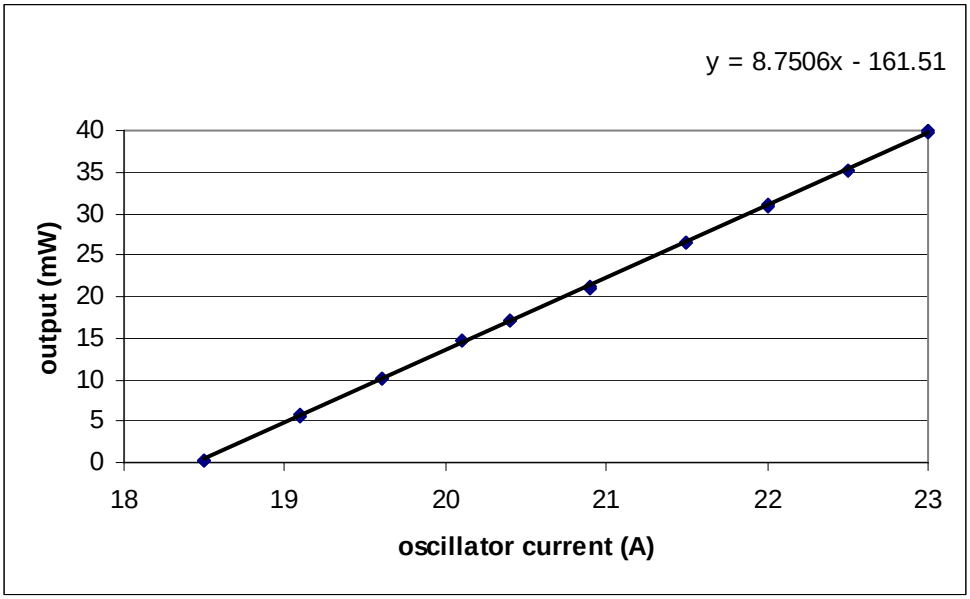

Figure 6: The oscillator laser (IR) output as the current is varied

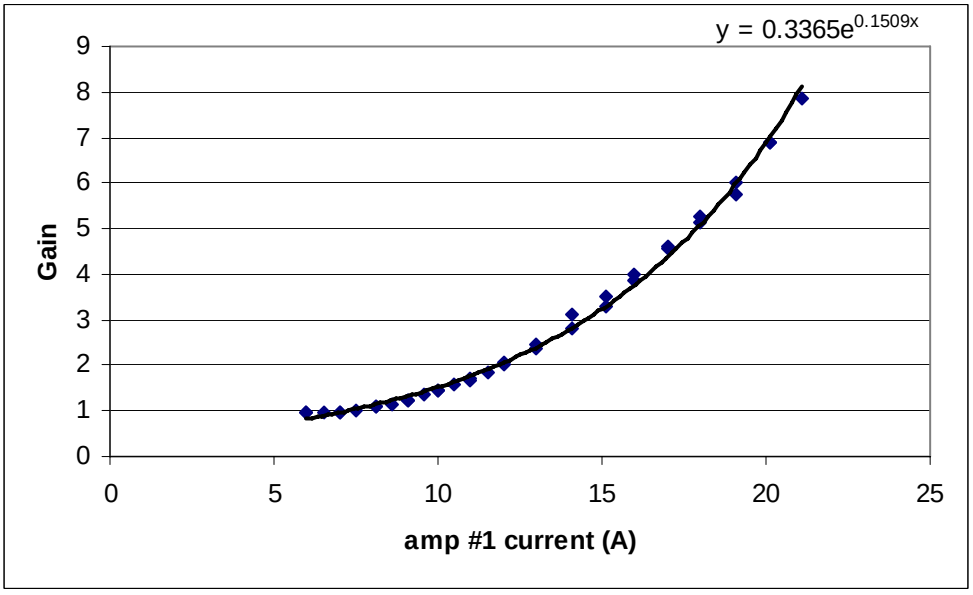

Figure 7: As the oscillator current was held constant at 23 amps, amplifier #1 current was varied from 6 to 21 amps. The graph of the gain versus the current of amplifier #1 reveals an exponential curve.

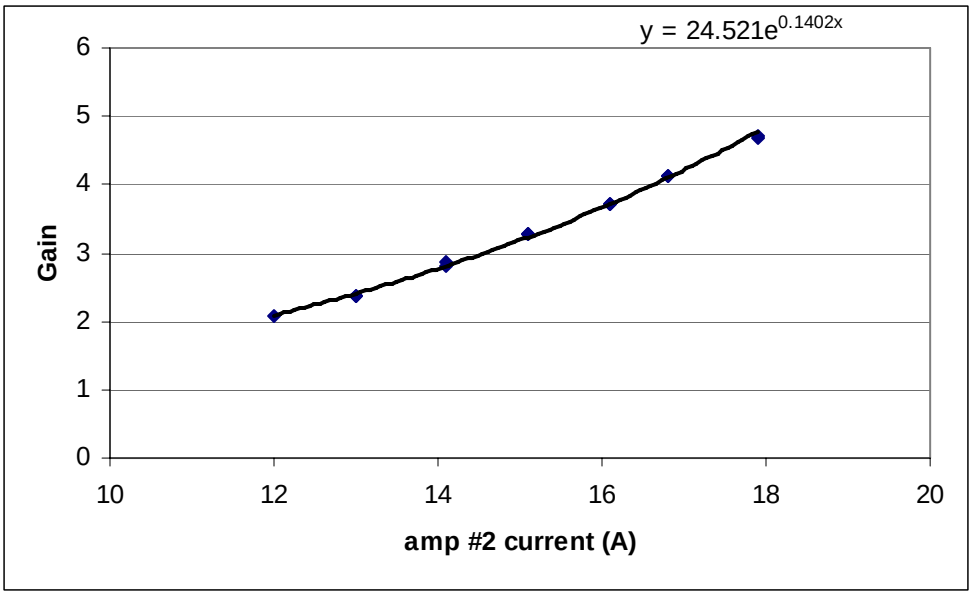

Figure 8: As the current for the oscillator and amplifier #1 was held constant (23 amps and 21 amps respectively), amplifier #2's current was varied from 12 to 18 amps. The graph displays an exponential curve for the gain versus current of amplifier #2.

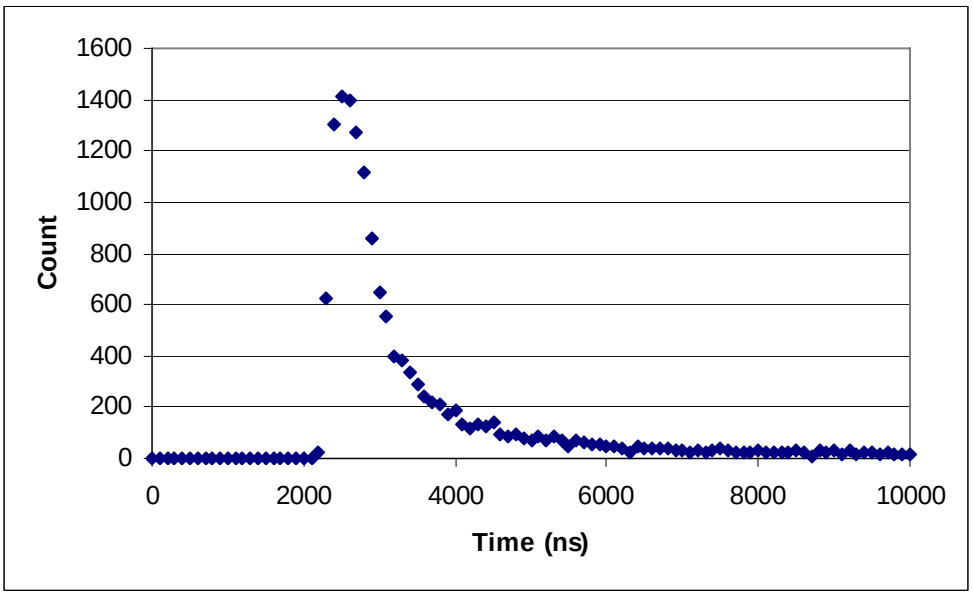

Figure 9: A sample of a pulse signal from the photomultiplier tube (Hamamatsu R7207) for the far-field UV

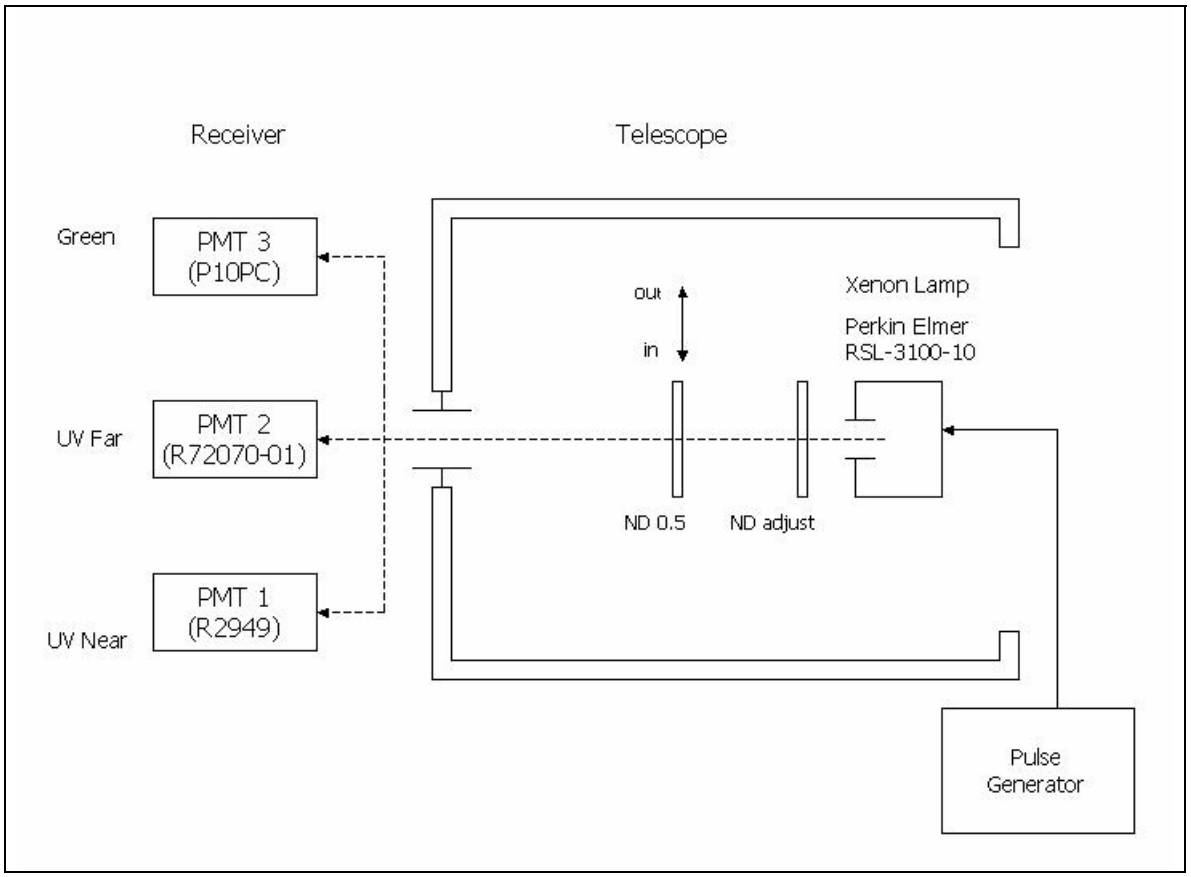

Figure 10: A diagram of the saturation measurement test setup. Note neutral density filters were added as needed to increase the xenon lamp's output range.

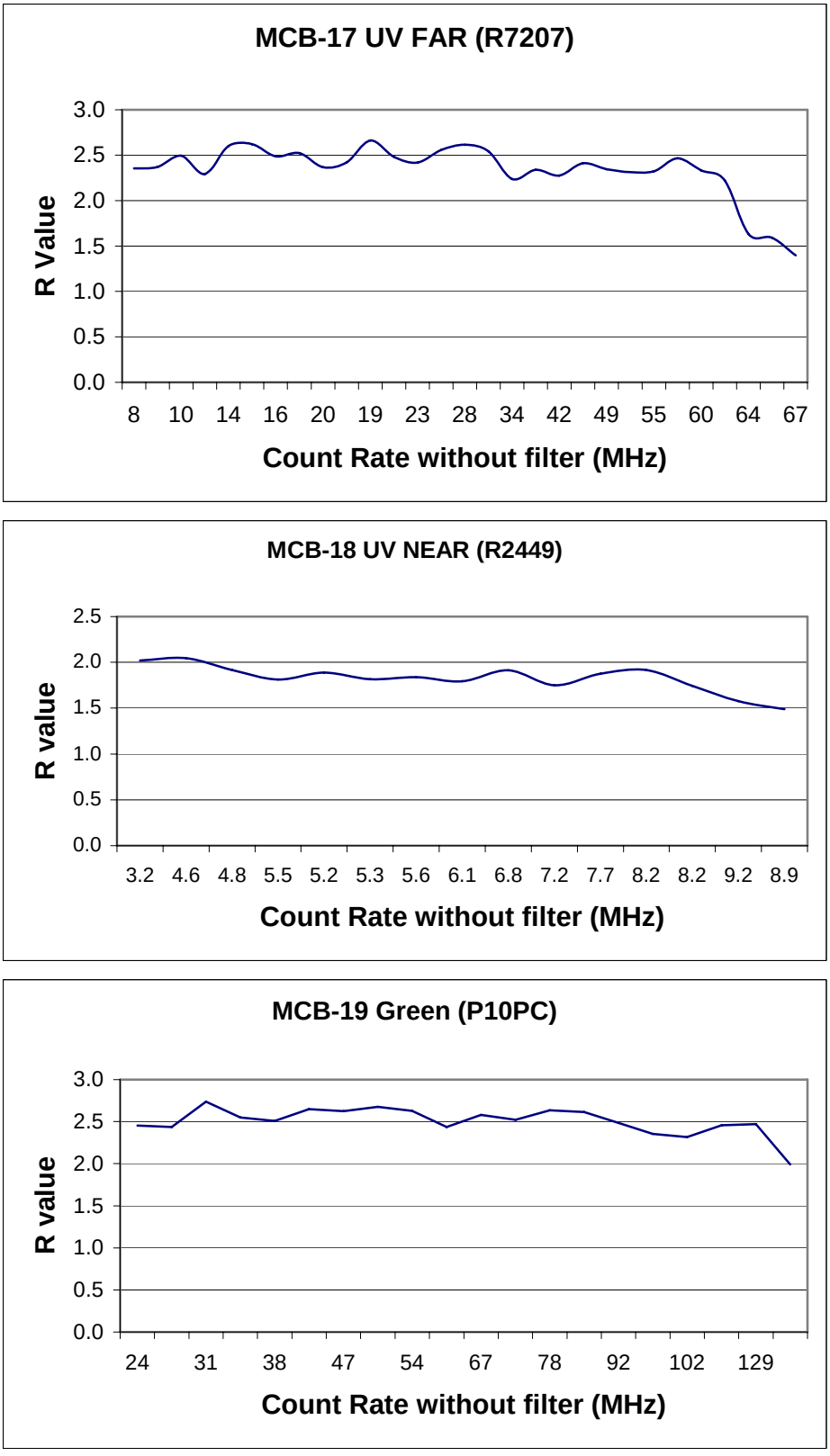

Figure 11: The three graphs display the maximum operating frequency (no saturation) for each photomultiplier tube. Two regions are displayed a linear region and a drop-off region. The drop-off represents the maximum frequency before saturation.

5.0 REFERENCES

1. Fishman, Jack. "Tropospheric Ozone." Handbook of Weather, Climate, and Water: Atmospheric Chemistry, Hydrology, and Societal Impacts. Thomas D. Potter and Bradley R. Colman. John Wiley & Sons, 2003.

2. Kaye, Jack, and Jack Fishman. "Stratospheric Ozone." Handbook of Weather, Climate, and Water: Atmospheric Chemistry, Hydrology, and Societal Impacts. Thomas D. Potter and Bradley R. Colman. John Wiley & Sons, 2003.

3. El-Sharkawi, Mohamed A. Electric Energy. New York: CRC Press, 2005.

4. NASA Facts. "Ozone: What is it, and why do we care about it?" NF-198. Greenbelt, Maryland. December 1993.

5. Mobile DIAL Lidar Operations Manual. Science and Engineering Services, Inc. Burtonsville, MD. June 2000. DoD contract #FO4611-99-C-0022.

6. Hamamatsu. Photon Counting. Photomultiplier Tubes: Basics and Applications. Third Edition. 2006 http://sales.hamamatsu.com/assets/applications/ETD/pmt_handbook/pmt_handbook_complete.pdf

7. Browell, Edward V.; "Differential Absorption Lidar Sensing of Ozone" Proceedings of the IEEE, Vol. 77, No. 3, March 1989.

REPORT DOCUMENTATION PAGE

Form Approved
OMB No. 0704-0188

1. REPORT DATE *(DD-MM-YYYY)*	2. REPORT TYPE	3. DATES COVERED *(From - To)*
01- 03 - 2007	Technical Memorandum	

4. TITLE AND SUBTITLE

Compact Ozone Lidar for Atmospheric Ozone and Aerosol Measurements

5a. CONTRACT NUMBER

5b. GRANT NUMBER

5c. PROGRAM ELEMENT NUMBER

6. AUTHOR(S)

Marcia, Joel; and De Young, Russell J.

5d. PROJECT NUMBER

5e. TASK NUMBER

5f. WORK UNIT NUMBER

7. PERFORMING ORGANIZATION NAME(S) AND ADDRESS(ES)

NASA Langley Research Center
Hampton, VA 23681-2199

8. PERFORMING ORGANIZATION REPORT NUMBER

L-19321

9. SPONSORING/MONITORING AGENCY NAME(S) AND ADDRESS(ES)

National Aeronautics and Space Administration
Washington, DC 20546-0001

10. SPONSOR/MONITOR'S ACRONYM(S)

NASA

11. SPONSOR/MONITOR'S REPORT NUMBER(S)

NASA/TM-2007-214544

12. DISTRIBUTION/AVAILABILITY STATEMENT

Unclassified - Unlimited
Subject Category 36
Availability: NASA CASI (301) 621-0390

13. SUPPLEMENTARY NOTES

An electronic version can be found at http://ntrs.nasa.gov

14. ABSTRACT

A small compact ozone differential absorption lidar capable of being deployed on a small aircraft or unpiloted atmospheric vehicle (UAV) has been tested. The Ce:LiCAF tunable UV laser is pumped by a quadrupled Nd:YLF laser. Test results on the laser transmitter demonstrated 1.4 W in the IR and 240 mW in the green at 1000 Hz. The receiver consists of three photon-counting channels, which are a far field PMT, a near field UV PMT, and a green PMT. Each channel was tested for their saturation characteristics.

15. SUBJECT TERMS

Lidar; Differential Absorption Lidar; DIAL; Ozone

16. SECURITY CLASSIFICATION OF:			17. LIMITATION OF ABSTRACT	18. NUMBER OF PAGES	19a. NAME OF RESPONSIBLE PERSON
a. REPORT	b. ABSTRACT	c. THIS PAGE			STI Help Desk (email: help@sti.nasa.gov)
					19b. TELEPHONE NUMBER *(Include area code)*
U	U	U	UU	21	(301) 621-0390